Effect of Poly(ethylene oxide) Homopolymer and Two Different Poly(ethylene oxide-*b*-poly(propylene oxide)-*b*-poly(ethylene oxide) Triblock Copolymers on Morphological, Optical, and Mechanical Properties of Nanostructured Unsaturated Polyester

Daniel H. Builes,[§,‡] Juan P. Hernández-Ortiz,[†,⊥] Mª Angeles Corcuera,[§] Iñaki Mondragon,[§] and Agnieszka Tercjak*,[§]

[§]Group 'Materials + Technologies', Polytechnic School, Dpto. Ingeniería Química y M. Ambiente, University of Basque Country (UPV/EHU), Pza. Europa 1, 20018 Donostia-San Sebastián, Spain

[‡]Research and Development Center 'DENOVO', Andercol S.A., 39290 Medellín, Colombia

[†]Department of Chemical and Biological Engineering, University of Wisconsin-Madison, Madison, Wisconsin 53706, United States

[⊥]Departamento de Materiales, Universidad Nacional de Colombia, Sede Medellín, 39290 Medellín, Colombia

S *Supporting Information*

ABSTRACT: Novel nanostructured unsaturated polyester resin-based thermosets, modified with poly(ethylene oxide) (PEO), poly(propylene oxide) (PPO), and two poly(ethylene oxide-*b*-propylene oxide-*b*-ethylene oxide) block copolymers (BCP), were developed and analyzed. The effects of molecular weights, blocks ratio, and curing temperatures on the final morphological, optical, and mechanical properties were reported. The block influence on the BCP miscibility was studied through uncured and cured mixtures of unsaturated polyester (UP) resins with PEO and PPO homopolymers having molecular weights similar to molecular weights of the blocks of BCP. The final morphology of the nanostructured thermosetting systems, containing BCP or homopolymers, was investigated, and multiple mechanisms of nanostructuration were listed and explained. By considering the miscibility of each block before and after curing, it was determined that the formation of the nanostructured matrices followed a self-assembly mechanism or a polymerization-induced phase separation mechanism. The miscibility between PEO or PPO blocks with one of two phases of UP matrix was highlighted due to its importance in the final thermoset properties. Relationships between the final morphology and thermoset optical and mechanical properties were examined. The mechanisms and physics behind the morphologies lead toward the design of highly transparent, nanostructured, and toughened thermosetting UP systems.

KEYWORDS: *unsaturated polyester, block copolymer, self-assembly, fracture toughness, transparency, micelles, thermosets*
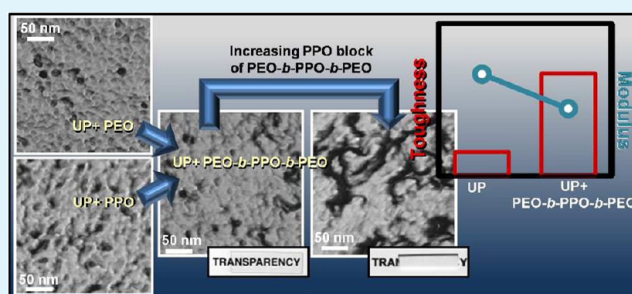
INTRODUCTION

Engineering thermosetting materials is an important area of research and development in material science, engineering, and industry. Its applications range from automotive and aerospace industries to novel nanoscale and supramolecular material design.[1−3] Unsaturated polyester (UP) resins are among the most common used resins for composites and thermosets, comprising more than 80% of the global market.[4] They offer high benefit−cost ratio and high Young's modulus, as they can be processed by simple and cost-effective setups. The addition of conventional thermoplastic polymers in UP resins improves the low toughness of the UP thermosets,[5−7] although a radical decreased optical transparency of the final material is the main drawback of the obtained materials. To overcome this drawback, in the past decade, researchers have focused their attention on modifying thermosetting polymers at nanometer scale, as can be made by means of block copolymers (BCPs).

The pioneer work of Hillmyer et al.[8] proved the possibility to design nanostructured thermosets using the ability of the BCPs to segregate in nanometric domains. In these systems, the thermosetting precursors could act as a solvent or as a selective solvent for the BCP. In the first case, polymerization-induced phase separation (PIPS) takes place,[9] and in the latter, the nanoscale structure is created by "frozen" self-assembled micelles formed before cross-linking.[10] This route to control the morphology of thermosets has been proved as an effective way to increase the toughness[1,11,12] or to modify optical properties.[13] Due to these advantages, a considerable amount of research is still focused on modifying properties of epoxy thermosetting systems.[10,14−23] In contrast, despite UP resins

are very commonly used, only a few works have been reported related to their nanostructuration employing BCPs. The first work was reported by Sinturel et al.,[24] who obtained lamellar structures in mixtures of an UP resin with a poly(ethylene-*b*-ethylene oxide) block copolymer. Later, Li et al.[25] proposed a method to study the domains interphase of a poly(ethylene oxide-*b*-propylene oxide-*b*-ethylene oxide) block copolymer mixed with an UP resin. On the other hand, Serrano et al.[26] synthetized BCPs based on poly(butyl acrylate) and the random poly(methyl methacrylate-co-N,N-dimethyl acrylamide) and studied their mixtures with a UP resin. Nevertheless, the last two research works did not pay attention to the morphology and optical transparency, and only the third work reported the mechanical properties of the designed thermosets.

In a previous work,[27] we reported an UP/poly(ethylene oxide-*b*-propylene oxide-*b*-ethylene oxide) (PEO-*b*-PPO-*b*-PEO) system with a marked effect of the lower critical solution temperature behavior (LCST) on nanostructure and optical transparency. The present work attempted to investigate the effect of curing conditions on morphology, optical transparency, and mechanical properties of UP-based thermosets modified with PEO homopolymer and two different PEO-*b*-PPO-*b*-PEO block copolymers with a noticeable difference of molar relation between blocks.

Differential scanning calorimetry (DSC), optical microscopy, and dynamic light scattering (DLS) were used to study the nonreactive mixtures in order to understand the miscibility behavior and the mechanisms of the morphology formation. The relationship between the final morphologies and the transparency of the designed thermosets were investigated using atomic force microscopy (AFM) and ultraviolet−visible spectroscopy (UV−vis), respectively. Finally, the mechanical properties by means of flexural modulus (E) and critical stress intensity factor (K_{Ic}) were studied.

■ EXPERIMENTAL SECTION

Materials and Chemicals. Linear poly(ethylene oxide-*b*-propylene oxide-*b*-ethylene oxide) (PEO-*b*-PPO-*b*-PEO) triblock copolymers with structures $E_{20}P_{69}E_{20}$ and $E_{75}P_{34}E_{75}$ were purchased from Sigma-Aldrich. The nomenclature is as follows: E for ethylene oxide and P for propylene oxide, while the subscripts indicate the number of repeated units. The BCPs have number average molecular weights (M_n) of 5750 and 8400 g/mol, respectively, denoted here as EPE20 and EPE75, respectively. Two commercial poly(propylene oxide) (PPO), with average number molecular weights of 2000 and 4000 g/mol (denoted as P34 and P69, respectively), and poly(ethylene oxide) (PEO), with 8000 and 3350 g/mol (denoted as E182 and E75, respectively), were provided by Sigma-Aldrich. The UP thermosetting precursor was a commercial UP resin with trade name Crystalan manufactured by Andercol S.A. It contained a prepolymer with a number average molecular weight (M_n) of 1800 g/mol and polydispersity index of 3 as determined by gel permeation chromatography, and it was composed of phthalic and maleic anhydrides and dissolved in styrene as cross-linking monomer with a C=C molar ratio between styrene and prepolymer of ca. 1. Methyl ethyl ketone peroxide (MEKP), supplied by Hegardt S.L., with the trade name Peroxan ME50L was used as polymerization initiator.

Blending Protocol. Nonreactive mixtures were prepared mixing UP resin with the corresponding modifier (EPE75, EPE20, etc.), followed by a constant stirring until a homogeneous liquid was obtained at room temperature (25 °C). Mixtures were denoted according to the modifier content in wt %. For example, the mixture named 15%E182 contained 15 wt % of E182 and 85 wt % of UP resin. UP oligomers (UPol), UPol/P34, and UPol/P69 mixtures were obtained by evaporation of styrene from thin films of UP/P34 or UP/69 mixtures, respectively, during two weeks in a vacuum oven at room

temperature. The reacting mixtures were prepared by adding 1.5 phr of MEKP (1.5 g of MEKP per 100 g of UP resin) at room temperature. The mold consists of two flat glasses separated by a U-shaped polytetrafluoroethylene (PTFE) sheet. Two isothermal curing cycles were carried out in a forced convection oven. In the first cycle, the mixtures were precured at 80 °C during 3 h and in the second at 60 °C during 7 h. The cycles were followed by a postcuring step of 3 h at 170 °C.

Differential Scanning Calorimetry (DSC). DSC measurements were performed in a Perkin-Elmer DSC-7 calorimeter under a helium flow of 10 mL min^{-1} as purge gas. Samples of approximately 15 mg were placed in 40 μL aluminum pans. The samples were first heated from 25 to 80 °C at 20 °C min^{-1}. Then, the samples were cooled from 80 to −95 °C at a rate of 1 °C min^{-1} followed by a second heating scan from −95 to 80 °C at a rate of 10 °C min^{-1}. Temperature was calibrated by using an indium standard. The temperature of the maximum point of an endothermic transition was taken as the melting temperature (T_m); the temperature of the minimum point of an exothermic transition was taken as the crystallization temperature (T_c), and the middle point of the slope change of the heat capacity plot was taken as the glass transition temperature (T_g).

Optical Microscopy. Measurements were carried out using a Nikon Eclipse E600W coupled with a hot stage Mettler FP 82 HT. Tests of transmitted light intensity were performed using a droplet of mixture introduced in a 1 mm thickness mold made of two coverslips and a flexible O-ring of PTFE.

Dynamic Light Scattering (DLS). DLS measurements were done in a Brookhaven BI-200SM goniometer with a 9000AT correlator. A light beam from a He−Ne laser (Mini L-30, wavelength λ = 637 nm, 10 mW) directed to a pot with a glass vat with a refractive index matching liquid surrounding the scattering cell and thermostatted at 25 and 80 °C was used. The scattered light intensity was measured at 90° with respect to the incident beam. A total of 256 ratio-spaced delay channels were used, with a sampling time of 20 μs, covering a delay time range from 20 μs to 200 ms. In order to avoid afterpulsing, the first correlation time channel was discarded during data analysis. The samples were prepared with a filtered UP resin. Each measurement was done during 10 min and repeated several times. Prior to the measurements, the samples were kept at room temperature around 48 h, which led to a considerable reduction of dust. The relaxation or decay rate (Γ) gives information about the dynamics of the mixture, viz., rapid diffusion of small particles leads to fast decay, while slow fluctuations result from the motions of larger particles.[28,29] Γ is defined as $\tau^{-1} = Dq^2$, where τ is the decay time, D is the diffusion coefficient, and $q = (4\pi n/\lambda)\sin(\theta/2)$ is the magnitude of scattering wave vector (where n is the refractive index of the medium, λ is the wavelength of the laser in a vacuum, and θ is the scattering angle).

Dynamic Mechanical Analysis (DMA). Dynamic mechanical analysis was done using a GABO Eplexor 100 N, with a three-point bending device having a span length of 20 mm. The loss factor (tan δ) was obtained by scans performed at a heating rate of 2 °C min^{-1} and a frequency of 10 Hz. Rectangular samples of 12.7 × 1.0 × 30 mm^3 were used.

Atomic Force Microscopy (AFM). Morphology of cured mixtures was analyzed using AFM with a scanning probe microscope (SPM) (NanoScope IIIa Multimode from Digital Instruments, Veeco Instruments, Inc.) in tapping mode. One beam cantilever (125 μm) with a silicon probe (curvature nominal radius of 5−10 nm) was used. Samples were prepared cutting an internal surface of the sheet using an ultramicrotome Leica Ultracut R with a diamond blade.

UV−Vis Measurements. UV−vis transmittance spectra of 1 mm thickness sheets of thermosetting mixtures were obtained at 25 °C using a spectrophotometer Shimadzu UV-3600 in the spectra range between 800 and 300 nm.

Mechanical Properties. Three-point bending and fracture toughness tests were performed following ASTM D 790-10 and ASTM D 5045-99 standards, respectively. A universal testing machine MTS model Insight 10, with a 250 N load cell was used. Rectangular samples of 12.7 × 1.0 × 40 mm^3 and a span length of 16 mm were

1074

dx.doi.org/10.1021/am4046266 | *ACS Appl. Mater. Interfaces* 2014, 6, 1073−1081

tested at a crosshead rate of 0.4 mm min^{-1} for flexural tests. Flexural modulus was determined from the slope of the load–displacement curve. The fracture toughness was evaluated in terms of the critical stress intensity factor (K_{Ic}). An approximate estimation of K_{Ic} values was obtained from a three-point bending test performed on single edge notched specimens (SENB). Rectangular samples of 6 × 1.5 × 30 mm^3 with 2.7 mm V-shaped notches and microcracks were tested at a crosshead rate of 10 mm min^{-1} and a span length of 23 mm. A minimum of five measurements were carried out per mixture.

■ RESULTS AND DISCUSSION

Miscibility of Nonreactive Mixtures. Miscibility and phase behavior of nonreactive mixtures of UP modified with 5–25 wt % of EPE75, EPE20, or E182 were analyzed. All investigated systems modified with 5–15 wt % were homogeneous and transparent at room temperature indicating the lack of macrophase separation at a visual wavelength scale. The increase of modifier content to 25 wt % generated changes in visual appearance only in the case of the UP/E182 system, which was solid and opaque at room temperature. DSC thermograms of UP/EPE75 and UP/E182 mixtures between 5 and 15 wt % are shown in Figure 1 and in the S1, Supporting
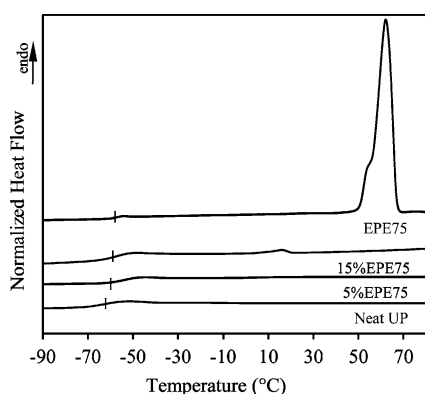

Figure 1. DSC thermograms during heating scan for nonreactive UP/EPE75 mixtures. The lines (|) denote the midpoints of the glass transition temperatures.

Information, respectively; thermal transition temperatures during cooling and heating scans are summarized in Table 1. Thermal transitions of UP/EPE20 mixtures were reported in our previous works.[27,30]

As is shown in Figure 1, the endothermic transition related to the melt of PEO and the T_m of UP/EPE75 mixtures decreased with the decrease of the modifiers content. This is common behavior for mixtures of crystalline/amorphous polymers with partial miscibility[31] and denoted that the UP resin hindered the

Table 1. DSC Thermal Transition Temperatures and Crystallization Degrees of Nonreactive UP/EPE75 and UP/E182 Mixtures

system	T_m (°C)	T_c (°C)	T_g (°C)	$X_{c\text{-PEO}}$ (%)
UP			−62	
EPE75	63	45	−58	75
15%EPE75	17		−59	1
5%EPE75			−60	
E182	73	51	−44	87
15%E182	27	−3	−55	39
5%E182			−56	

crystallization of PEO as a consequence of the formation of intermolecular hydrogen bonds between the ether oxygen of PEO and the hydroxyl groups of UP oligomers.[24,32] The crystallization degree of PEO ($X_{c\text{-PEO}}$) in UP/EPE75 and UP/E182 mixtures was calculated using the following equation[33] (see Table 1):

$$X_{c\text{-PEO}} = (\Delta H_f - \Delta H_c)/\Delta H^\circ_{f-PEO}$$

where ΔH°_{f-PEO} = 205 J/g is the heat of fusion of 100% crystalline PEO, ΔH_f is the specific heat of fusion, and ΔH_c is the specific heat of crystallization during the second heating scan. No additional crystallization was observed for any of the investigated mixtures during heating scans. As it is well-known from literature, due to the amorphous nature of PPO,[21] the crystallization degree and melting point of PEO-b-PPO-b-PEO triblock copolymers are lower than the melting point of PEO homopolymer. The different states and visual appearance of 25%EPE75 and 25%E182 mixtures was strongly related to this behavior of PEO-b-PPO-b-PEO triblock copolymers.

On the other hand, both UP/EPE75 and UP/E182 mixtures showed a T_g located between the T_gs of the neat components (see Table 1), indicating high miscibility between them. A different behavior was observed in nonreactive UP/EPE20 mixtures,[27] where two T_gs were detected outside of the range of the T_gs of neat components due to the formation of self-assembled micelles of EPE20. The high similitude between behaviors of nonreactive UP/EPE75 and UP/E182 mixtures indicates that the PPO block of EPE75 was miscible with the UP resin. According to this, it could be concluded that the molecular weight of the PPO central block of PEO-b-PPO-b-PEO allowed the BCPs miscibility of nonreactive UP/EPE75 and UP/EPE20 mixtures to switch from miscible to microphase separated, respectively. In order to study this phenomenon, miscibility between UP resin and PPO homopolymers with molecular weights similar to those of the central blocks of EPE75 and EPE20 was carried out. Figure 2 shows the detected
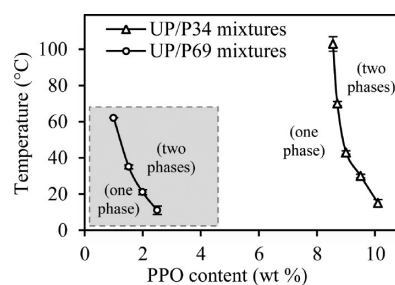

Figure 2. Temperature–PPO content phase diagram of nonreactive UP/PPO mixtures for: (−o−) UP/P69 and (−Δ−) UP/P34 systems. (one phase): transparent and homogeneous mixtures. (two phases): cloudy mixtures.

cloud points obtained by measuring the changes in transmitted light intensity of nonreactive UP/P34 and UP/P69 mixtures as a function of temperature and PPO content.

As can be seen, UP/PPO mixtures presented a LCST behavior[21,35] strongly influenced by the molecular weight of PPO. Miscibility between PPO and each one of components of the UP resin, viz., oligomers of unsaturated polyester (UPol) and styrene (St), was also analyzed. DSC measurements of UPol/P34 mixtures (see S2a, Supporting Information), which revealed a maximum miscibility threshold between 4 and 7 wt % of P34 content, revealed higher miscibility between

components than miscibility observed in UPol/P69 mixtures (see S2b, Supporting Information). In the case of PPO/St mixtures, almost complete miscibility at both molecular weights of PPO was observed. The above can be explained by considering the interaction parameters of PPO with UPol and PPO with St, with values of $\chi_{UPol-PPO} = 4.1$ and $\chi_{PPO-St} = 0.36$, respectively, calculated by the Hoftyzer and Van Krevelen method.[34] These values indicate weak contribution of UPol and strong contribution of St to the miscibility of PPO with UP resin. The last is in good agreement with the results reported in the literature.[35−38] Consequently, taking into account the phase diagram of Figure 2 and that the PPO block content in the 15% EPE75 mixture was ca. 3 wt %, it could be confirmed that no phase separation of PPO central block would take place in the UP/EPE75 mixtures from 25 to 80 °C. Likewise, for the UP/P69 mixtures, the maximum miscibility threshold at room temperature was lower than 2 wt %, corroborating the micelle formation in nonreactive 5%EPE20 mixture.[27] Furthermore, the phase diagram shown in Figure 2 points out that a mixture of UP with 1 wt % of P34 (the PPO content of the 5%EPE75 mixture) was miscible from 25 to 80 °C and suggests that the amphiphilicity of EPE75 in nonreactive UP resins was not sufficient to trigger self-assembled micelles.

Dynamics of Nonreactive Mixtures. A dynamics monitoring of UP resin and nonreactive 5%EPE75, 5%E182, and 5%EPE20 mixtures was performed by means of DLS from 25 to 80 °C. No intensity autocorrelation functions ($g_2(t)$) were obtained with the measurements performed for UP resin and 5%EPE75 and 5%E182 mixtures. This is a typical behavior of systems without particles or micelles and agrees with the high miscibility observed in DSC measurements for the nonreactive UP/EPE75 mixtures (see Figure 1). On the contrary, the 5%EPE20 mixture displayed $g_2(t)$ at 25 and at 80 °C, with a decay time that changed from $\tau q^2 = 1.1 \times 10^{13}$ to 1.5×10^{11} s m^{-2}, respectively (see S3, Supporting Information). This tendency of $g_2(t)$ to shift to lower relaxation times is indicative of a faster dynamic, which could be generated by smaller EPE20 micelles or by a reduction of viscosity of the UP resin.[39−41] It could be explained considering that miscibility of PEO blocks with UP resin decreases with the increase of temperature from 25 to 80 °C, generating a reduction of the extension of PEO chains. As a consequence, a reduction of corona diameter of micelles and also of the hydrodynamic diameter of micelles could be expected. Similar behavior was reported for PEO-b-PPO-b-PEO block copolymers in aqueous solutions,[39,42,43] where at low temperature (ca. <15 °C) PPO and PEO blocks were miscible and at ca. 25 °C water becomes a selective solvent, viz., PPO block phase separates and PEO blocks remain miscible. After an additional increase of temperature, the PEO lateral blocks also lose their miscibility and macrophase separation was reached. An extended comparison between behavior of aqueous solutions of PEO-b-PPO-b-PEO and UP resin mixed with PEO-b-PPO-b-PEO was reported in our previous work.[27]

Miscibility of Cured Mixtures. Mixtures of UP with 5 and 15 wt % of EPE75, E182, or EPE20 were cured at 80 and 60 °C and analyzed by optical microscopy and DMA. Only the 15% EPE20 cured mixture becomes opaque owing to macrophase separation, which is in agreement with results reported by Li et al.[25] Figure 3 shows the temperature dependence of the loss factor (tan δ) of the neat UP resin and for UP/EPE75, UP/E182, and UP/EPE20 mixtures with 15 wt % of modifier cured at 80 °C (the dynamic mechanical spectra including modulus
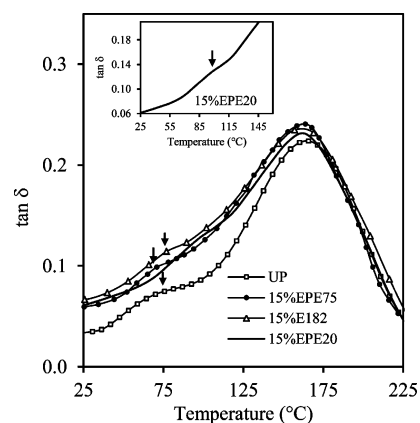

Figure 3. Loss factor (tan δ) curves as a function of temperature for: (−□−) UP, (−●−) 15%EPE75, (−Δ−) 15%E182, and (−) 15% EPE20 mixtures cured at 80 °C. The inset details the shoulder (signed by an arrow) in tan δ curve for 15%EPE20 thermoset.

(E') and loss factor (tan δ) versus temperature from −90 °C is shown in S4 Supporting Information. Curves at 60 °C were not included for brevity).

As can be seen, the tan δ peaks appear in a broad temperature range with a shoulder between 40 and 120 °C, which is typical of a UP matrix due to its two phases, i.e., polystyrene-rich and polyester-rich phases.[5,30] Temperatures of the maximum of tan δ peaks of the cured mixtures were ascribed to the glass transition temperature of polyester-rich matrix (T_{g-UP}) and the shoulders to polystyrene-rich phase. According to the Fox equation,[5] if UP resin and E182 were completely miscible, the T_{g-UP} would shift from 165 to 110 °C for the cured UP and 15%E182 mixture, respectively (Table 2).

Table 2. DSC Thermal Transitions Temperatures of the Thermosetting Systems Cured at 80 and 60 °C

system	T_{g-UP} (°C)[a]	T_{g-cold} (°C)[b]	T_m (°C)[b]
	cured at 80 °C		
UP	165		
15%EPE75	163	−50	41
15%E182	161	−43	50
15%EPE20	162	−63	23
	cured at 60 °C		
UP	162		
15%EPE75	160	−50	
15%E182	161	−45	
15%EPE20	162	−64	

[a]Data from DMA results (see Figure 3). [b]Data from DSC results (see Figure 4).

Thus, due to the T_{g-UP} of cured mixtures being almost that of the neat UP, it could be concluded that components were immiscible at this curing condition. A weak variation of T_g of the matrix after being modified with BCPs containing PEO-miscibile blocks was also reported in epoxy systems.[15] Nevertheless, the DMA spectra of Figure 3 showed a noticeable increase in the height of tan δ curve at temperatures lower than T_{g-UP}. This could be explained considering the mixing of a part of modifiers with the cross-linked UP-rich phase provoking a higher mobility of it.[16]

On the other hand, the variation observed for the temperature of shoulders (ca. 76 °C for UP and 15%E182
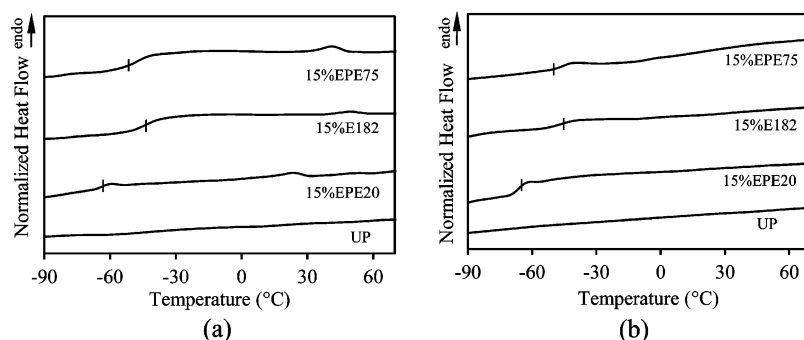
Figure 4. DSC thermograms of UP and 15%EPE75, 15%E182, and 15%EPE20 mixtures cured at (a) 80 °C and (b) 60 °C. The lines (|) denote the midpoints of the glass transition temperatures.

and 70 and 97 °C for 15%EPE75 and 15%EPE20, respectively) suggests that the investigated modifiers affected selectively both phases of the UP matrix. This effect was also observed by Dong et al.[44] in a UP resin modified with several homopolymers.

The thermal behavior of cured mixtures at lower temperatures was analyzed by DSC. Figure 4 shows the thermal transitions of neat UP and its modification with 15 wt % of EPE75, E182, or EPE20 cured at 80 °C (Figure 4a) and at 60 °C (Figure 4b). As can be seen, the mixtures displayed a T_g at low temperatures ($T_{g\text{-cold}}$) and a melting peak only in the case of the systems cured at 80 °C. These temperatures are summarized in Table 2.

The $T_{g\text{-cold}}$s of 15%E182 and 15%EPE20 mixtures were equal to the T_gs of the neat E182 (Table 1) and EPE20,[27] respectively, indicating that the mixtures had a separated phase. However, the $T_{g\text{-cold}}$ of 15%EPE75 mixture presented a value between the T_gs of the EPE75 and the neat UP thermoset, which could imply that the separated phase was a mixture between a block of EPE75 and a phase of UP thermoset. These DSC results are in agreement with results reported in the literature.[25] The last constituted a new fact that indicates that EPE75 had higher miscibility than E182 with UP resin. These differences in miscibility were also observed in the visual appearance of nonreactive 25%EPE75 and 25%E182 mixtures and can be justified due to the PPO central block preventing crystallization of PEO. These DSC results indicated also that curing at lower temperature allowed the crystallization of PEO in the mixtures to be hindered, which means that it was provoked by higher polymer–polymer interactions between PEO and UP network.

Morphology Analysis of Cured Mixtures. Internal surfaces of the fully cured mixtures were trimmed using an ultramicrotome, and the sections were used to analyze the morphology by means of atomic force microscopy (AFM). The AFM images shown in Figure 5 depicted the morphology of neat UP resin and 5%EPE75, 5%E182, and 5%EPE20 mixtures cured at 80 °C (see S5 and S6, Supporting Information, for morphology of mixtures cured at 60 °C).

Figure 5a shows the sphere-like nanostructure obtained in the UP matrix, which can be justified considering that curing a UP resin generates microphase separation of cross-linked UPol from St and generates a heterogeneous network of polyester-rich phase surrounded by polystyrene-rich phase.[5] The morphologies shown in Figure 5b–d show that, besides the nanostructure of the UP matrix, a second sphere-like nanostructure owing to the microphase separation of modifiers was generated. Taking into account the DSC and DLS analysis for nonreactive UP/EPE75 and UP/E182 mixtures, where no
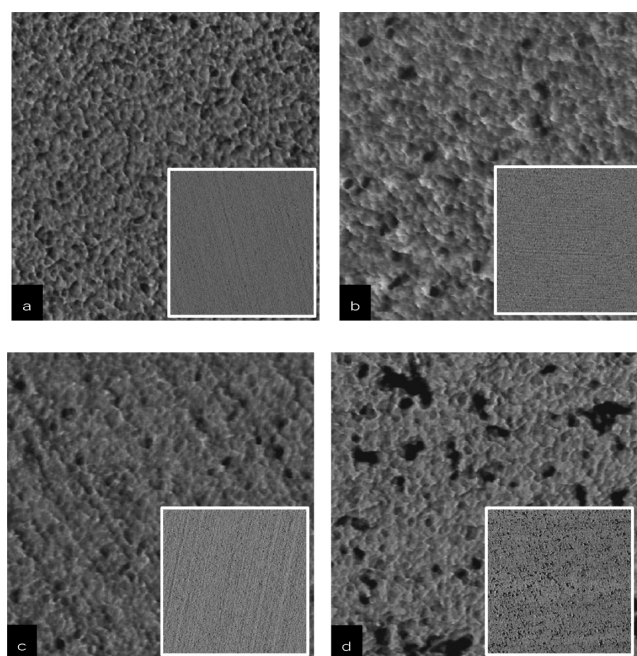

Figure 5. AFM images (0.5 μm × 0.5 μm) of (a) neat UP, (b) 5% EPE75, (c) 5%E182, and (d) 5%EPE20 cured at 80 °C. The insets correspond to 3 μm × 3 μm AFM images. This AFM image corresponds to internal surfaces of the cured mixtures trimmed using an ultramicrotome.

phase separation was detected, it could be concluded that the final morphologies shown in Figure 5b,c for 5%EPE75 and 5% E182 cured mixtures, respectively, were driven by polymerization-induced phase separation (PIPS) due to the weak miscibility of PEO and a cross-linked UP network.[25] The last contrast with the self-assembly mechanism followed by the 5% EPE20 cured mixture to reach the morphology observed in Figure 5d.[27]

The effect of increasing the modifiers content to 15 wt % on the morphology of cured mixtures was also studied. The morphologies achieved for 15%EPE75, 15%E182, and 15% EPE20 mixtures cured at 80 °C are shown in Figure 6. Microphase separation was clearly distinguished for 15%EPE75 and 15%E182 cured mixtures and macrophase separation for the 15%EPE20 cured mixture. The increment of EPE75 content drove the morphology of the UP/EPE75 mixture to evolve from sphere-like to worm-like domains. A similar evolution in morphology was observed in other systems,[9,45] and it was explained through the combination of mechanisms such
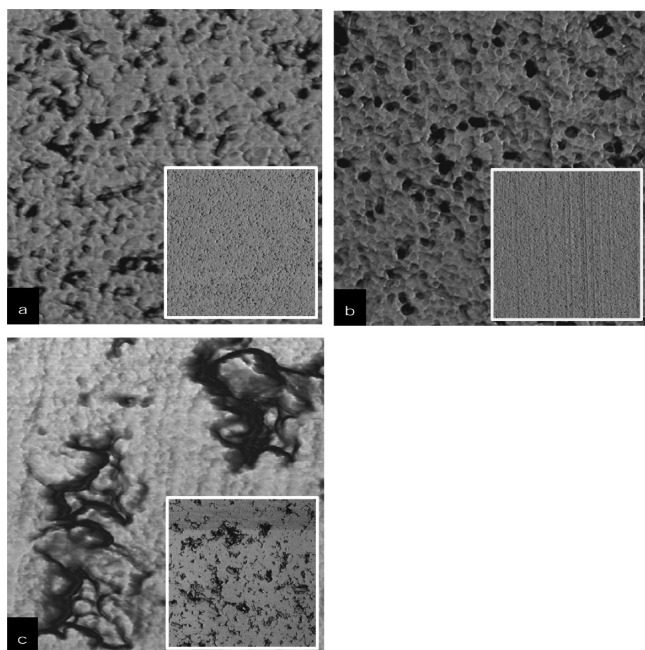
Figure 6. AFM phase images (0.5 μm × 0.5 μm) of 15 wt % modified thermosets cured at 80 °C for: (a) 15%EPE75, (b) 15%E182, and (c) 15%EPE20 mixtures. The insets correspond to 3 μm × 3 μm AFM images. These AFM images correspond to internal surfaces of the cured mixtures trimmed using an ultramicrotome.

as coalescence and elongation—distortion of the spherical micelles. On the other hand, increasing the PEO content in the UP/E182 mixture resulted in well-defined sphere-like domains. This strong phase separation of PEO explains the almost unchanged $T_{\text{g-UP}}$ of UP/E182 mixtures (Figure 3) and the increase of the height of the tan δ curve suggesting a thin interphase surrounding the microphase separated domains of E182. This interface was studied elsewhere for the case of PEO-b-PPO-b-PEO triblock copolymers mixed with UP[25] or epoxy thermosets.[46] Regarding the 15%EPE20 mixture, macrophase separation generated by coalesced worm-like domains can be clearly distinguished (Figure 6c).

The morphology of UP/EPE75 and UP/E182 cured mixtures observed in Figures 5 and 6 allowed us to understand the morphology achieved for UP/EPE20 cured mixtures. The morphology of the 5%EPE20 cured mixture simultaneously exhibited a sphere-like structure and elongated domains (see Figure 5d). UP/EPE20 morphology was driven by both self-assembled micelles stabilized by the PEO lateral blocks[27] and simultaneously suffered phase separation of the PEO blocks during cross-linking. Consequently, one can conclude that at this curing condition the coalescence is encouraged owing to a reduction of steric stabilization[42] and an increase in collisions of micelles (i.e., higher particle dynamics; see S3, Supporting Information). Thus, the formation of macrophase separated structures could be favored for higher EPE20 content as can be observed for the 15%EPE20 cured mixture (Figure 6c). A similar phenomenon was observed for PEO/PPO BCPs mixed with epoxy resins.[17]

To study the influence of PEO and PPO blocks of the EPE75 block copolymer on the morphology of the 15%EPE75 mixture, the morphology of 12%E75 and 3%P34 mixtures cured at 80 °C was also analyzed (see Figure 7). The last two mixtures were prepared with PEO and PPO homopolymers with similar

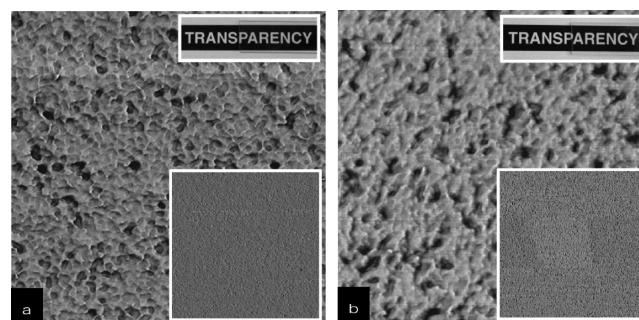contents and molecular weights of the PEO and PPO blocks in the 15%EPE75 mixture.

Figure 7. AFM phase images (0.5 μm × 0.5 μm) of (a) 12%E75 and (b) 3%P34 mixtures cured at 80 °C. The insets at the top of each image correspond to the digital image of transparency of a sheet of 1 mm of thickness. The insets at the bottom correspond to 3 μm × 3 μm AFM images. These AFM images correspond to internal surfaces of the cured mixtures trimmed using an ultramicrotome.

As can be noted, the 12%E75 mixture (Figure 7a) exhibited a sphere-like morphology whereas the 3%P34 mixture (Figure 7b) showed a tendency to form worm-like phase separated domains. Subsequently, comparing the morphologies of 15% EPE75 and 15%E182 cured mixtures (see Figure 6a,b, respectively), one could conclude that the worm-like morphology of 15%EPE75 was associated with the presence of PPO central block. This effect is more noticeable when molecular weight and content of PPO central block are higher (see the morphology of the 15%EPE20 cured mixture in Figure 6c).

Five wt % modified mixtures cured at 60 or 80 °C presented almost no differences in morphology. On the contrary, a size reduction of ca. 35% was observed in 15%EPE75 and 15%E182 mixtures if cured at 60 °C. Regarding the 15%EPE20 mixture cured at 60 °C, despite a macrophase separation being observed, the phase separated domains were smaller and more segregated (see S6c, Supporting Information). The last temperature dependence of the morphology of the mixtures was directly related to temperature dependence of miscibility in the PEO-UP resin system.

Figure 8 shows a schematic explanation of the morphology obtained for cured mixtures as a function of curing temperature. Since PEO miscibility with UPol[33] is higher than miscibility with St, it is expected that during the cross-linking process PEO remains inside UP-rich microgels (white circles) as sphere-like domains (dark gray circles) surrounded by an interface (light gray), which becomes thinner at higher curing temperatures (see right side of Figure 8a).

On the other hand, taking into account that P34 showed partial miscibility with UPol and St (see Figure 2 and S2a, Supporting Information), P34 nanodomains (black ovals in Figure 8b) could remain partially in the microgels and/or be surrounded by the polystyrene-rich phase depending on the curing temperature and P34 content. Hence, considering the structure of EPE75 (i.e., $E_{75}P_{34}E_{75}$), it is expected that UP/EPE75 cured mixtures present a combination of the effects observed in Figure 8a,b (see Figure 8c). In the case of EPE20 (with structure $E_{20}P_{69}E_{20}$), one could expect that PPO always remained outside of the microgels due to its high immiscibility with UPol (see S2b, Supporting Information). Furthermore,
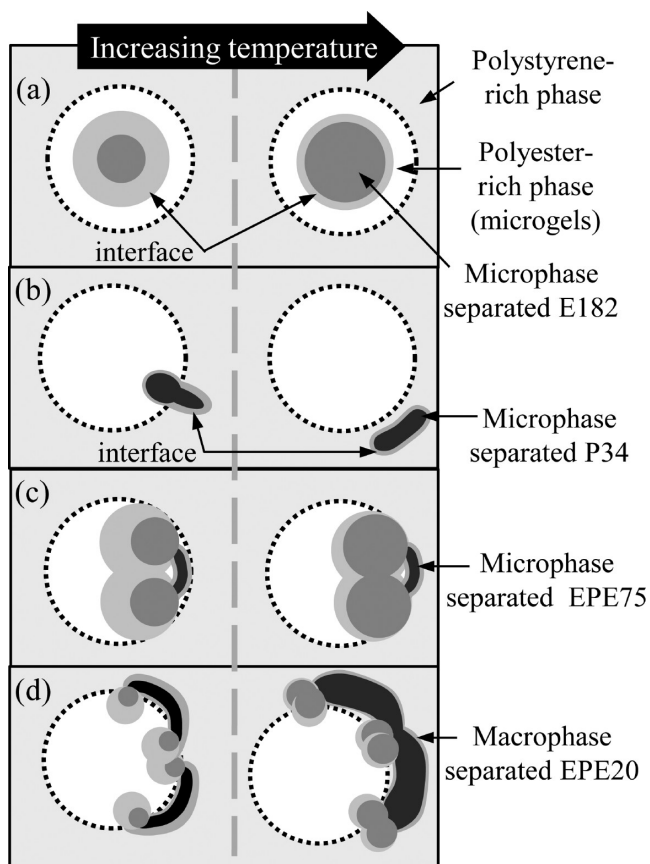
Figure 8. Schematic representation of morphology achieved by UP matrix modified with (a) E182, (b) P34, (c) EPE75, and (d) EPE20. Right side corresponds to mixtures cured at higher temperatures than the left side.

the increase of the temperature generates the self-assembled micelles coalescence and generates macrophase separation (Figure 8d).

Optical Transparency of Cured Mixtures. In order to examine the effects of the modifiers content and curing temperature on the optical transparency, UV−vis measure-ments at wavelengths from 800 to 300 nm were performed. Figure 9 shows regular light transmittance of UV−vis spectra and the visual appearance for UP/EPE75, UP/E182, and UP/EPE20 cured mixtures.

As can be observed, transmittance of cured mixtures decreased with the increase of modifiers content following a similar tendency of other composites.[27,47,48] This phenomenon can be explained considering that the light extinction through the thermosetting sheets occurs by matter absorption and the scattering due to heterogeneities or/and refractive index fluctuations[49,50] which increase with the increase of modifier content. As shown in Figure 9a, UP/E182 cured mixtures exhibited higher transparency, which indeed was slightly higher than UP transmittance at wavelengths from 800 to 500 nm. Regarding the effect of curing temperature, a tendency of the mixtures modified with 5 wt % to reach higher light transmittance when cured at 60 °C than at 80 °C was observed. This effect could have a relationship with the increase of size domains produced by the increase of curing temper-ature, as was observed in UP/EPE20 mixtures at EPE20 content from 5 to 50 wt %.[27] The same behavior with curing temperature was observed in the 15%E182 cured mixture and the opposite in 15%EPE75. This could be related to the fact that EPE75, unlike E182 and EPE20, is composed with a PPO block that can be miscible with both phases of UP matrix (see Figure 8c). This selective miscibility, which depends on the curing temperature and EPE75 content, could generate fluctuations in refractive index in one or another phase of the matrix in the proximity of the interface of microphase separated domains.

Mechanical Properties. Mechanical properties of cured mixtures were investigated measuring flexural modulus (E) and the critical stress intensity factor (K_{Ic}). Figure 10 shows values of E (Figure 10a) and K_{Ic} (Figure 10b) as a function of modifier content and curing temperature.

Mixtures modified with 5 wt % showed weak differences of E varying both the modifier and the curing temperature. A reduction of E was expected due to the lower modulus of incorporated PEO-composed modifiers and the fact that the new phase remained as free dangling chains.[51,52] Increasing the modifier content to 15 wt % reduced the magnitude of E in a
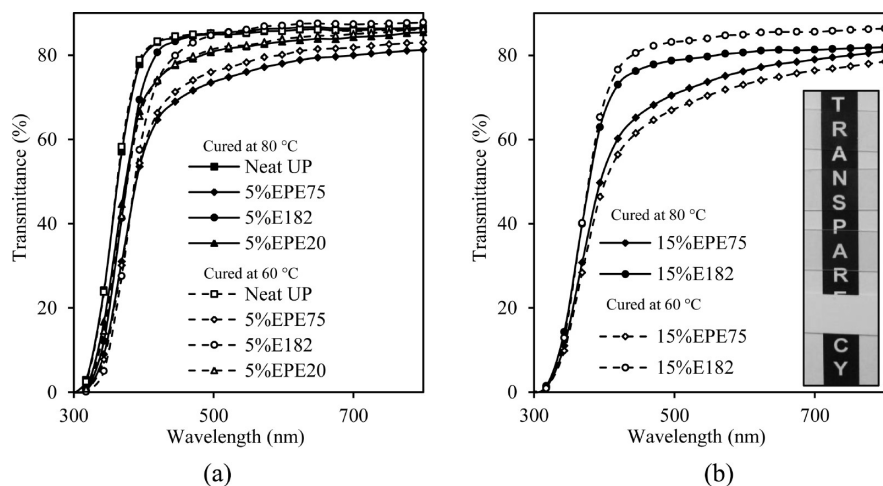

Figure 9. Regular transmittance of UV−vis spectra of mixtures cured at 80 °C (filled symbols) and 60 °C (open symbols) for: (a) UP and mixtures with 5 wt % of modifier content and (b) mixtures with 15 wt % of modifier content. The inset of (b) corresponds to the digital image of sheets of 1 mm thickness for (from up to bottom): UP and 15%E182, 15%EPE75, and 15%EPE20 mixtures cured at 80 °C.
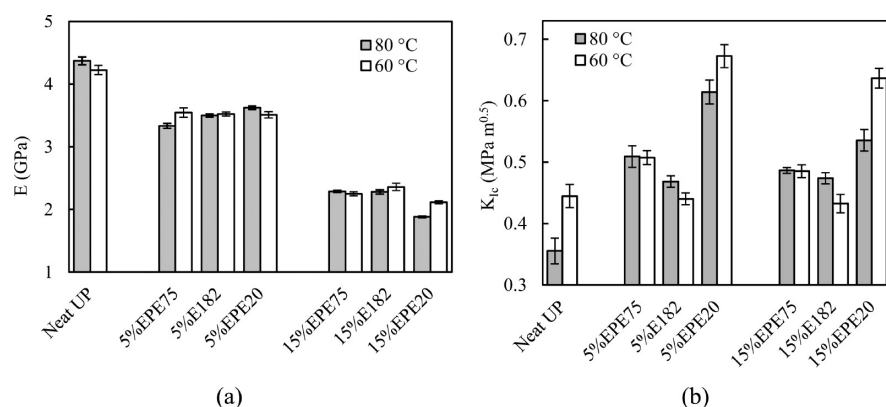
Figure 10. Mechanical properties of investigated thermosetting mixtures as a function of the modifier content and curing temperature. (a) Flexural modulus, E, and (b) critical stress intensity factor, K_{Ic}.

similar ratio for both mixtures modified with EPE75 and E182. The lower values of E were observed for the 15%EPE20 mixtures cured at 80 or 60 °C, which were strongly related to their macrophase separation. Furthermore, according to the morphology analysis, it can be noted that the 15%EPE20 mixture cured at 80 °C exhibited the biggest domains and the lowest E.

On the other hand, it was proved that all modifiers could toughen the UP matrix. The K_{Ic} values of 5 wt % modified mixtures showed an incremental tendency in function of quantity and size of phase separated domains. The dependence of dispersion, size, and shape of the microstructure on toughness of the cured mixtures has been reported in the literature.[10,18,19] Similarly to the works presented in the literature, 5%EPE75 and 5%EPE20 mixtures exhibited higher fracture toughness and also higher quantity and size of phase separated domains (see Figures 10b and 5b−d) pointing out that PPO block was favorable to improve fracture toughness. This effect increased with the increase of PPO molecular weight. Thus, a higher K_{Ic} value was observed for the 5%EPE20 mixture cured at 60 °C (i.e., 0.67 MPa m$^{0.5}$), and the highest improvement was observed for this mixture cured at 80 °C (i.e., 70% if compared with UP matrix cured at the same temperature). Finally, it could be highlighted that the effect of curing temperature on fracture toughness was stronger for UP/EPE20 systems. This effect was expected as a consequence of temperature sensibility of dispersion of EPE20 in UP resin due to the low molecular weight and content of PEO-stabilizer blocks.

CONCLUSIONS

Two poly(ethylene oxide-*b*-propylene oxide-*b*-ethylene oxide) block copolymers, with different molecular weight and ratio between blocks, and a poly(ethylene oxide) homopolymer were used as modifiers for unsaturated polyester in order to fabricate nanostructured thermosetting materials. Novel conclusions about the effect of the PPO central block of BCPs and curing temperature on morphology and optical properties were listed. Partial miscibility of PPO and PEO homopolymers with the UP resin in cured and uncured systems were analyzed, and their relationship with the morphology and mechanisms of nanostructuration with BCPs were explained. It was found that PPO central block could be miscible or phase separated before curing depending on its molecular weight leading the nanostructuration of the matrix by means of self-assembly or polymerization induced phase separation mechanisms. Selective

miscibility of blocks of BCPs with the two phases of the UP matrix was found, and the effects on morphology, transparency, and mechanical properties were analyzed. Fracture toughness measurements revealed that PPO block was favorable to improve fracture toughness, which the effect of increased with the increase of PPO molecular weight. Improvements in K_{Ic} higher than 70% if compared with UP matrix cured at the same temperature using 5 wt % of EPE20 were obtained.

Characteristics of blocks of BCPs, curing temperature, and/or matrix chemistry are variables that allow the design and fabrication of different types of thermosetting materials. Proper selection of these variables could induce two different mechanisms to drive the nanostructuration of the matrix, which can be used separately or synergistically depending on the desired properties of the final nanocomposite. This design strategy of materials contributes to a proper control of final morphology of these nanostructured thermosetting systems that can be used to better understand the relation between morphology and final optical and mechanical properties.

ASSOCIATED CONTENT

Ⓢ Supporting Information

DSC thermograms during heating scan for nonreactive UP/E182 mixtures. DSC thermograms of UPol/P34 and UPol/P69 mixtures at several PPO contents from 0 to 100 wt %. Dynamic mechanical spectra including modulus (E') and loss factor (tan δ) versus temperature from −90 °C for UP, 15%EPE75, 15% E182, and 15%EPE20 mixtures cured at 80 °C. Intensity correlation function versus time for the 5%EPE20 nonreactive mixture at 25 and 80 °C. AFM images of mixtures modified with 5 and 15 wt % of E182, EPE75, and EPE20 cured at 60 °C. This information is available free of charge via the Internet at http://pubs.acs.org/.

AUTHOR INFORMATION

Corresponding Author

*E-mail: agnieszka.tercjaks@ehu.es. Tel.: +34 943 017 169. Fax: +34 943 017 130.

Notes

The authors declare no competing financial interest.

ACKNOWLEDGMENTS

■ DEDICATION

This work is dedicated to the memory of Prof. Iñaki Mondragon (1954−2012), who founded the "Materials + Technologies" Group in 1988 and who passed away after his contribution to this work.

■ REFERENCES

(1) Ruzette, A. V.; Leibler, L. *Nat. Mater.* **2005**, *4*, 19−31.
(2) Suhr, J.; Koratkar, N.; Keblinski, P.; Ajayan, P. *Nat. Mater.* **2005**, *4*, 134−137.
(3) De Volder, M. F.; Tawfick, S. H.; Baughman, R. H.; Hart, A. J. *Science* **2013**, *339*, 535−539.
(4) *Global Unsaturated Polyester Resin Market 2010−2015*, 2010, Lucintel Market Reports Page. http://www.lucintel.com/marketglobalUPRtrend.aspx (accessed Dec 10, 2013).
(5) Pascault, J. P.; Sautereau, H.; Verdu, J.; Williams, R. J. J. In *Thermosetting polymers*; Marcel Dekker: New York, 2002.
(6) Bakar, M.; Djaider, F. *J. Thermoplast. Compos. Mater.* **2007**, *20*, 53−64.
(7) De la Caba, K.; Guerrero, P.; Gavalda, J.; Mondragon, I. *J. Polym. Sci., Part B: Polym. Phys.* **1999**, *37*, 1677−1685.
(8) Hillmyer, M.; Lipic, P.; Hajduk, D.; Almdal, K.; Bates, F. *J. Am. Chem. Soc.* **1997**, *119*, 2749−2750.
(9) Meng, F.; Xu, Z.; Zheng, S. *Macromolecules* **2008**, *41*, 1411−1420.
(10) Ocando, C.; Tercjak, A.; Martín, M. D.; Ramos, J. A.; Campo, M.; Mondragon, I. *Macromolecules* **2009**, *42*, 6215−6224.
(11) Redline, E. M.; Francis, L. F.; Bates, F. S. *J. Polym. Sci., Part B: Polym. Phys.* **2011**, *49*, 540−550.
(12) Ruiz-Pérez, L.; Royston, G. J.; Fairclough, J. P. A.; Ryan, A. J. *Polymer* **2008**, *49*, 4475−4448.
(13) Thomas, S.; Harrats, C.; Groeninckx, G. In *Micro- and nanostructured multiphase polymer blends systems. Phase morphology and interfaces*; Harrats, C., Thomas, S., Groeninckyx, G., Eds.; CRC Taylor and Francis Group: Boca Raton, 2006; p 25.
(14) Guo, Q.; Thomann, R.; Gronski, W. *Macromolecules* **2002**, *35*, 3133−3144.
(15) Liu, J.; Thompson, Z. J.; Sue, H. J.; Bates, F. S.; Hillmyer, M. A.; Dettloff, M.; Jacob, G.; Verghese, N.; Pham, H. *Macromolecules* **2010**, *43*, 7238−7243.
(16) Liu, J.; Sue, H.; Thompson, Z.; Bates, F.; Dettloff, M.; Jacob, G.; Verghese, N.; Pham, H. *Acta Mater.* **2009**, *57*, 2691−2701.
(17) Larrañaga, M.; Arruti, P.; Serrano, E.; de la Caba, K.; Remiro, P. M.; Riccardi, C. C.; Mondragon, I. *Colloid Polym. Sci.* **2006**, *284*, 1419−1430.
(18) Dean, J. M. E.; Lipic, P. M.; Cook, R. F.; Bates, F. S. *J. Polym. Sci., Part B: Polym. Phys.* **2001**, *39*, 2996−3010.
(19) Dean, J. M.; Grubbs, R. B.; Saad, W.; Cook, R. F; Bates, F. S. *J. Polym. Sci., Part B: Polym. Phys.* **2003**, *41*, 2444−2456.
(20) Zheng, S. Nanostructured Epoxies by the Use of Block Copolymers. In *Epoxy Polymers: New Materials and Innovations*; Pascault, J. P., Williams, J. J., Eds.; Wiley-VCH: Weinheim, Germany, 2010.
(21) Larrañaga, M.; Gabilondo, N.; Kortaberria, G.; Serrano, E.; Remiro, P.; Riccardi, C. C.; Mondragon, I. *Polymer* **2005**, *46*, 7082−7093.
(22) Larrañaga, M.; Martin, M. D.; Gabilondo, N.; Kortaberria, G.; Corcuera, M. A.; Riccardi, C. C.; Mondragon, I. *Polym. Int.* **2004**, *53*, 1495−1502.
(23) Larrañaga, M.; Martin, M. D.; Gabilondo, N.; Kortaberria, G.; Eceiza, A.; Riccardi, C. C.; Mondragon, I. *Colloid Polym. Sci.* **2006**, *284*, 1403−1410.
(24) Sinturel, C.; Vayer, M.; Erre, R.; Amenitsch, H. *Macromolecules* **2007**, *40*, 2532−2538.
(25) Li, X.; Fu, W.; Wang, Y.; Chen, T.; Liu, X.; Lin, H.; Sun, P.; Jin, Q.; Ding, D. *Polymer* **2008**, *49*, 2886−2897.
(26) Serrano, E.; Gerard, P.; Lortie, F.; Pascault, J. P.; Portinha, D. *Macromol. Mater. Eng.* **2008**, *293*, 820−827.
(27) Builes, D. H.; Hernandez, H.; Mondragon, I.; Tercjak, A. *J. Phys. Chem. C* **2013**, *117*, 3563−3571.
(28) Borkovec, M. Measuring Particle Size by Light Scattering. In *Handbook of Applied Surface and Colloid Chemistry*; Holmberg, K., Shah, D., Schwuger, M., Eds.; John Wiley & Sons, Ltd.: Chichester, 2002; p 357−370.
(29) Schärtl, W. *Light Scattering from Polymer Solutions and Nanoparticle Dispersions*; Springer-Verlag: Berlin,, 2007; p 8−24.
(30) Builes, D. H.; Tercjak, A.; Mondragon, I. *Polymer* **2012**, *53*, 3669−3676.
(31) Guo, Q.; Thomann, R.; Gronski, W. *Macromolecules* **2003**, *36*, 3635−3645.
(32) Zheng, H.; Zheng, S.; Guo, Q. *J. Polym. Sci., Part A: Polym. Chem.* **1997**, *35*, 3169−3179.
(33) Zheng, H.; Zheng, S.; Guo, Q. *J. Polym. Sci., Part A: Polym. Chem.* **1997**, *35*, 3161−3168.
(34) Van Krevelen, D. W.; Te Nijenhuis, K. In *Properties of Polymers*, 4th ed.; Elsevier: Amsterdam, 2009; p 201.
(35) Boyard, N.; Sinturel, C.; Vayer, M.; Erre, R. *J. Appl. Polym. Sci.* **2006**, *102*, 149−165.
(36) Drohmann, C.; Beckman, E. J. *J. Supercrit. Fluids* **2002**, *22*, 103−110.
(37) Matynia, T.; Worzakowska, M.; Tarnawski, W. *J. Appl. Polym. Sci.* **2006**, *101*, 3143−3150.
(38) Sun, M. C.; Chang, Y. F.; Yu, T. L. *J. Appl. Polym. Sci.* **2001**, *79*, 1439−1449.
(39) Kostko, A. F.; Harden, J. L.; McHugh, M. A. *Macromolecules* **2009**, *42*, 5328−5338.
(40) Kjøniksen, A. L.; Nyström, B.; Lindman, B. *Colloids Surf., A* **1999**, *149*, 347−354.
(41) Liu, R.; Gao, X.; Oppermann, W. *Polymer* **2006**, *47*, 8488−8494.
(42) Hamley, I. In *Block Copolymers in Solution: Fundamentals and Applications*; John Wiley & Sons: Chichester, 2005; p 18.
(43) Chen, S.; Yang, B.; Guo, S.; Ma, J. H.; Yang, L. R.; Liang, X.; Hua, C.; Liu, H. Z. *J. Phys. Chem. B* **2008**, *112*, 15659−15665.
(44) Dong, J. P.; Huang, J. G.; Lee, F. H.; Roan, J. W.; Huang, Y. J. *J. Appl. Polym. Sci.* **2004**, *91*, 3369−3386.
(45) Ramos, J. A.; Espósito, L.; Fernández, R.; Zalakain, I.; Goyanes, S.; Avgeropoulos, A.; Zafeiropoulos, N. E.; Kortaberria, G.; Mondragon, I. *Macromolecules* **2012**, *45*, 1483−1491.
(46) Sun, P.; Dang, Q.; Li, B.; Chen, T.; Wang, Y.; Lin, H.; Jin, Q.; Ding, D. *Macromolecules* **2005**, *38*, 5654−5667.
(47) Tao, P.; Viswanath, A.; Schadler, L.; Benicewicz, B.; Siegel, R. *ACS Appl. Mater. Interfaces* **2011**, *3*, 3638−3645.
(48) Zhang, H.; Qi, R.; Tong, M.; Su, Y.; Huang, M. *J. Appl. Polym. Sci.* **2012**, *125*, 1152−1160.
(49) Boyard, N.; Serre, C.; Vayer, M. *J. Appl. Polym. Sci.* **2007**, *103*, 451−461.
(50) Willmouth, F. M. In *Optical Properties of Polymers*; Meeten, G. H., Ed.; Elsevier Applied Science Publishers: London, 1986; p 286.
(51) Schulze, U.; Skrifvars, M.; Reichelt, N.; Schmidt, H. *J. Appl. Polym. Sci.* **1997**, *64* (3), 527−537.
(52) Pandit, S.; Nadkarni, V. *Ind. Eng. Chem. Res.* **1994**, *33*, 2778−2788.